Available online at www.sciencedirect.com
SCIENCE DIRECT®
Journal of Solid State Chemistry 178 (2005) 2186–2190
JOURNAL OF SOLID STATE CHEMISTRY
www.elsevier.com/locate/jssc

The effect of Ag addition on electrical properties of the thermoelectric compound $Ca_3Co_4O_9$

M. Mikami[a,b,*], N. Ando[a], R. Funahashi[a,b]

[a]National Institute of Advanced Industrial Science and Technology, 1-8-31, Midorigaoka, Ikeda, Osaka 563-8577, Japan
[b]CREST, Japan Science and Technology Agency, 4-1-8, Honcho Kawaguchi, Saitama 332-0012, Japan

Received 7 February 2005; received in revised form 19 April 2005; accepted 24 April 2005
Available online 23 May 2005

Abstract

$Ca_3Co_4O_9$/Ag composites incorporating different amounts of Ag were synthesized by solid-state reaction. Scanning electron microscopy revealed Ag particles dispersed among and combined with $Ca_3Co_4O_9$ grains several times larger in size. The electrical resistivity (ρ) of the composites is favorably lower than that of $Ca_3Co_4O_9$ alone and decreases with increasing Ag content. It can thus be inferred that the highly conductive Ag particles between the oxide grains contribute to the reduction of ρ. Although minimal in smaller amounts, the addition of Ag also seems to have a negative impact on the Seebeck coefficient (S) of the composites due to its poor S. Since the reduction of ρ is more significant than the degradation of S, the power factor is found to be improved by the addition of 10 wt% Ag.

Keywords: Oxide; Layered cobaltite; Composite; Thermoelectric properties

1. Introduction

Thermoelectric devices have recently attracted renewed interest for their potential application to clean energy-conversion systems. The conversion efficiency of a thermoelectric material is expressed by the figure of merit $Z = S^2/\rho\kappa$, where S is the Seebeck coefficient, ρ is the electrical resistivity, and κ is the thermal conductivity. Materials to be used for a thermoelectric device should thus have a large S and, at the same time, low ρ and κ values. For practical applications, thermoelectric materials need to have a dimensionless figure of merit ZT (where T is absolute temperature) greater than 1. Moreover, they should be harmless to the environment and chemically stable in air at high temperatures for power generation from waste heat in higher temperature regions (e.g. such as 627–1773 K in the steel industry and 473–1223 K in the ceramic industry). The recent discovery of large S coexisting with low ρ in the layered cobaltites Na_xCoO_2 and $Ca_3Co_4O_9$ (Co349) has opened the way to the exploration of thermoelectric oxide materials, which are generally stable at high temperatures in air [1–5]. The single crystal of these cobalt oxides exhibits good thermoelectric performance along the *ab*-plane ($ZT > 1$ at 1000 K [2,4]), which is competitive with that of conventional degenerate semiconductors such as Bi_2Te_3, PbTe, and $Si_{1-x}Ge_x$.

However, the ZT of randomly oriented polycrystalline materials is rather small because of the highly anisotropic properties of these layered cobaltites [6,7], though some partial element substitutions enhance ZT of bulk Co349 [8–10]. Texturization of polycrystalline bulk material is therefore indispensable for the realization of ZT high enough for practical applications, as it is difficult to grow single crystals large enough for the construction of a thermoelectric device. With this objective, some research groups have already reported

*Corresponding author. National Institute of Advanced Industrial Science and Technology, 1-8-31, Midorigaoka, Ikeda, Osaka 563-8577, Japan. Fax: +81 72 751 9622.
E-mail address: m-mikami@aist.go.jp (M. Mikami).

0022-4596/$ - see front matter © 2005 Elsevier Inc. All rights reserved.
doi:10.1016/j.jssc.2005.04.027

the successful fabrication of textured Co349 ceramics by way of reactive templated grain growth [11–13], magnetic alignment [14–16] and utilization of the combined effect of large single crystals and powder [17]. The authors have also demonstrated the validity of using large-grained Co349 powder as material for producing textured Co349 ceramics [18]. The resulting textured samples show reduced ρ values comparable to non-aligned, sintered Co349 materials.

Despite the progress made ρ values of well-aligned ceramics are still about two times larger along the *ab*-plane than those of single crystal materials. Consequently, Z values of textured ceramics are less than half those intrinsic to Co349. Therefore, we should modify not only the grain alignment but also electron scattering at grain boundaries in order to decrease the ρ values of polycrystalline materials. Since Co349 does not melt but decomposes at high temperatures, it is difficult to reduce the number of grain boundaries by adjusting the sintering or annealing conditions (i.e. by the partial melting technique). On the other hand, it is expected that the addition of a material, which has a lower ρ than cobaltite, at the grain boundaries would be effective to reduce the electrical resistance at the grain boundary. For instance, the addition of fine metallic particles would form electrically connected grains in a cobaltite/metal composite material. Based on this concept, it has recently been reported that the addition of Ag to polycrystalline Na_xCoO_2 can successfully reduce ρ and consequently improve the thermoelectric power factor ($PF = S^2/\rho$) [19]. In the present study, we examined the effect of Ag addition on the thermoelectric properties of Co349 bulk materials.

2. Experimental

Co349 powder was prepared by solid-state reaction. A mixture of Co_3O_4 (99.9%) and $CaCO_3$ (99.5%) in a molar ratio of Ca:Co = 3:4 was ground, calcined at 1073 K for 10 h in air, pulverized, and pressed into pellets, which were then sintered at 1153 K for 20 h in an oxygen gas flow and ground into fine powder. In order to increase the grain size, the obtained Co349 powder was then heated at 1123 K for 20 h in a 20 wt% solvent of K_2CO_3 and KCl in a molar ratio of 4:1 [18]. The powder was collected from the solidified materials by dissolving the solvent in distilled water using an ultrasonic cleaner.

The large-grained powder was mixed with fine Ag_2O powder in four different weight ratios to Co349:0 wt% (without Ag_2O), 5, 10, and 20 wt%. As seen in Fig. 1, although Ag_2O grains of 3–4 μm in size can be found, the major portion of Ag_2O particles is less than 1 μm, which is considerably smaller than the Co349 grains of several μm in size. Since fine particles of Ag readily stick together and agglomerate during the mixing process, Ag_2O was used and seems to be favorable as a source for dispersal of Ag particles in the synthesized composites. The mixtures were cold-pressed into 15 thin disks, which were finally stacked under uniaxial pressure of 180 MPa. These laminated pellets were then hot-forged at 1153 K for 20 h in air under uniaxial pressure of 10 MPa. The obtained samples were cut into bars with a typical size of $2.5 \times 2.5 \times 10\,mm^3$ for the measurement of transport properties. In the present paper, the hot-forged samples prepared from the large-grained Co349 powders mixed with the Ag_2O of 0, 5, 10, and 20 wt% are abbreviated as CA-0, -5, -10, and -20, respectively.

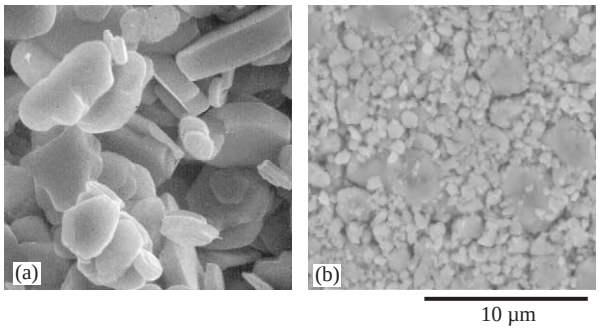

Fig. 1. SEM images of (a) large-grained Co349 powder and (b) Ag_2O powder.

Crystallographic structure analysis was performed by X-ray diffraction (XRD) using Cu$K\alpha$ radiation. The microstructures of the samples were observed with a scanning electron microscope (SEM) using both secondary electron and back-scattered electron (BSE) modes. The constituent analysis was conducted using an energy-dispersive X-ray spectrometer (EDX). ρ was measured in air in the temperature range of 300–1073 K using a conventional four-probe DC technique. S was calculated from a plot of thermoelectric voltage against temperature differential as measured in air at 373–1073 K using an instrument designed by our laboratory. Two Pt–Pt/Rh (R-type) thermocouples were attached to both ends of the sample using Ag paste, and the Pt wires of the thermocouples were used as voltage terminals. Measured S values were reduced by those of the Pt wires alone to obtain the net S values of the samples.

3. Results and discussion

XRD measurement was performed on the pressed surfaces of hot-forged samples. As shown in Fig. 2, the XRD patterns of all samples agree with the reported data for Co349 structure [6], except for weak diffraction peaks from the secondary phase of Ag (marked •) in the Co349/Ag composites. No impurity phase such as K_2CO_3 or KCl contained in the solvent of the grain

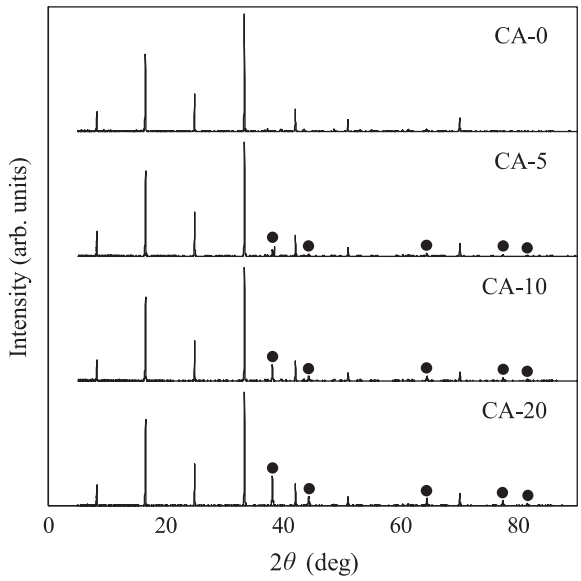

Fig. 2. XRD patterns (Cu$K\alpha$ radiation) of hot-forged Co349 and Co349/Ag samples. Measurement was performed on the polished pressed plane. Diffraction peaks in each XRD pattern can be assigned to the Co349 structure except for weak diffraction peaks from the secondary phase of Ag (marked •).

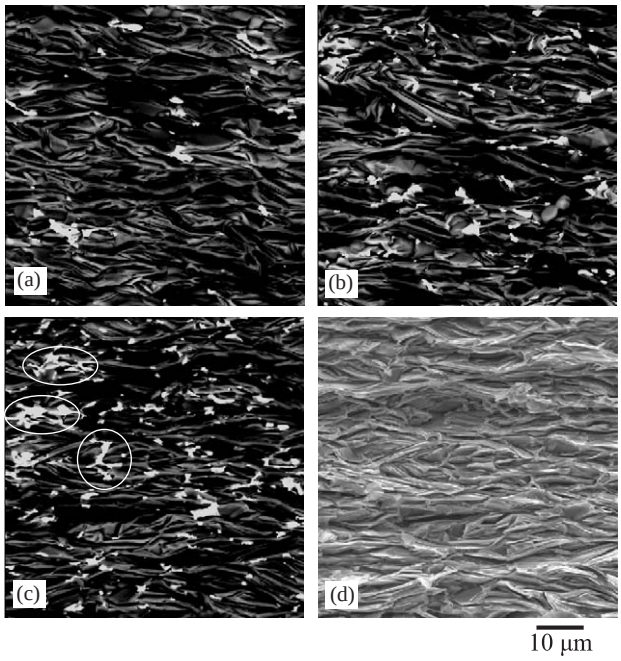

Fig. 3. BSE images of fractured cross-sections of Co349/Ag composites containing (a) 5 wt%, (b) 10 wt%, and (c) 20 wt% of Ag. White spots in the BSE images correspond to Ag particles. (d) An SEM image of a fractured cross-section of Co349/Ag composite at 20 wt%. Almost the same microstructure was observed in other hot-forged samples.

growth procedure and no diffraction peak from unreacted compound such as $CaCO_3$ or Co_3O_4 were observed. Since strong peaks in each XRD pattern can be assigned to a 00l peak of Co349 structure, it can be inferred that the *ab*-plane in the cobaltite grains is well aligned parallel to the pressed plane. In addition, the intensity ratio between 00l peaks and other diffraction peaks attributed to Co349 structure is almost the same in each sample. Thus, the degree of orientation of the cobaltite grains seems not to be affected by the amount of Ag. The 2θ angles of 00l peaks are slightly increased, less than 0.02°, by the Ag addition. Because Ag was not detected by EDX in the Co349 grains, we hypothesize that this slight peak shift does not derive from Ag substitution for Ca and/or Co sites, but rather from the difference in the number of oxygen defects in the Co349 structure, which has relatively high number of oxygen vacancies [20,21], due to the oxidation effect of Ag_2O. In other words, Ag_2O might compensate the intrinsic oxygen vacancies in Co349. Additional analysis of oxygen content is needed to confirm this hypothesis. Since all of the Ag-related peaks agree with those of Ag in metal form, it is confirmed that Ag_2O used as starting material was reduced by the hot-forging process. Moreover, the intensity of the Ag peaks clearly increases with the increase of the mixed ratio of Ag_2O.

Fig. 3 shows SEM and BSE images of fractured cross-sections of the composites. White spots in the BSE images (Figs. 3(a)–(c)) correspond to Ag particles. It can be observed that the cobaltite grains of several micrometers in size are well aligned as predicted from the XRD patterns in CA-20 (Fig. 3(d)). It should be mentioned that a similar degree of orientation and grain size was observed in other samples. On the other hand, the amount of Ag particles apparently increases with the increase of the mixed ratio of Ag_2O in the starting powder. Although the average size of the Ag particles seems to be almost the same in each composite, the number of conjoined Ag particles (see in the white circles of Fig. 3(c)) seems to increase with the increase in Ag content. Although agglomerated Ag particles of several micrometers in size can be found, the major portion of Ag particles is less than 3 μm. In addition, Ag particles are dispersed and Ag particles larger than 10 μm could not be found. As listed in Table 1, it was confirmed by EDX analysis that the content of Ag in each composite was almost the same as the initial amount of Ag_2O in the starting powder. This Ag weight ratio was calculated based on the reported oxygen composition of Co349 phase: Co:O = 4.00:9.30 [20,21]. The slight increase in Ag content is mainly attributed to measurement error in the EDX analysis. In addition, the incorporation of K or Cl contained in the solvent of the grain growth process was not detected. From these results, it was verified that the four samples have almost the same microstructure but different Ag content.

As shown in Fig. 4, the average ρ value is reduced according to the Ag content. The T dependence of ρ also changes with the amount of Ag added. ρ of CA-0

Table 1
Atomic ratios of samples measured by EDX and calculated weight ratios of Ag based on the reported oxygen content of Co:O = 4.00:9.30 in Co349 [17,18]

	Atomic ratio			Ag weight ratio (%)
	Ca	Co	Ag	
CA-0	2.99	4.00	—	—
CA-5	3.10	4.00	0.14	5.6
CA-10	3.05	4.00	0.28	10.6
CA-0	2.99	4.00	0.59	20.0

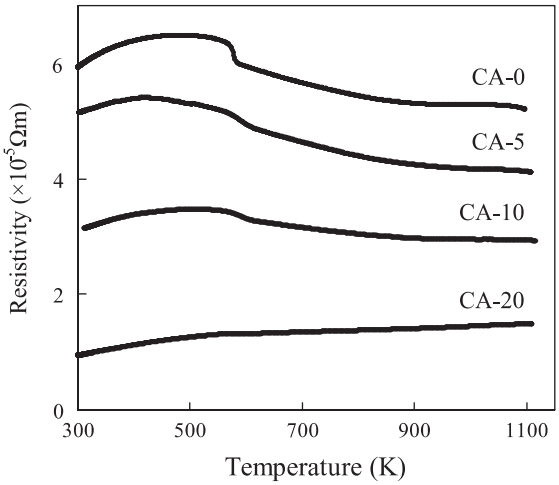

Fig. 4. T dependence of ρ along the pressed plane of hot-forged Co349 and Co349/Ag samples.

gradually decreases with the increase of temperature except for a broad maximum around 500 K and a steep decline at 570 K. A broad hump around 500 K could correspond to the behavior of ρ in the single-crystal Co349 along the *ab*-plane [5]. However, since a steep decrease around 570 K is only observed in hot-forged polycrystalline samples, the rapid reduction could be related to ρ along the *c*-axis or to the electrical properties of the grain boundaries. The reduction rate of ρ with the increase in temperature tends to decline with the increase in the Ag content. CA-20 eventually exhibits metallic T behavior ($d\rho/dT > 0$) over the entire measured temperature range. These results clearly indicate that the ρ of the Co349/Ag composite consists of the semiconducting behavior of Co349 and the metallic behavior of Ag.

As shown in Fig. 5, the S value of each sample increases with increasing temperature. This T dependence is similar to single-crystal Co349. Contrary to the Ag concentration dependence of ρ, the addition of Ag has little affect on S, with the exception of CA-20, where S is less than half what it is in CA-0. Since the S of Ag in metal form is low, less than 10 μV/K, it seems obvious to assume that S is reduced by the addition of Ag as Ag_2O.

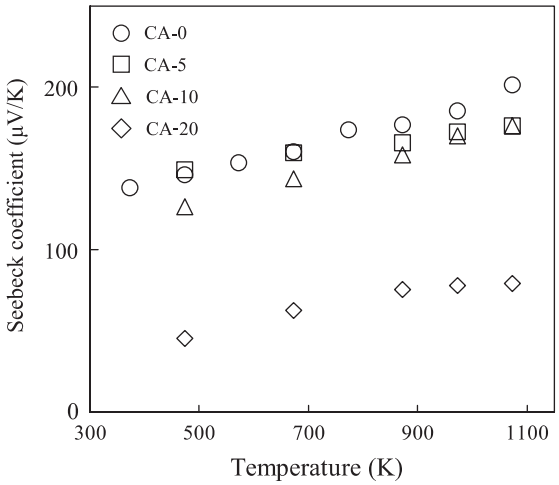

Fig. 5. T dependence of S along the pressed plane of the hot-forged Co349 and Co349/Ag composites.

However, the difference in the degree of impact on the S of CA-20 and other composites due to Ag addition requires further explanation. We propose that Ag particles play two roles in a composite: (1) as electrical connections between cobaltite grains and (2) as bypasses in carrier transport. It is presumed that the former has little influence on S, because the thermoelectric power voltage of each Co349 grain is additive like the elements of a series circuit. In its latter role, however, Ag can nullify the thermoelectric voltage of Co349 grains like a short-circuited power source. If the Ag particles are well separated and quite small compared to the oxide grains, the latter effect could be negligible. Conversely, if the Ag particles are close to each other or agglomerated into particles larger than the Co349 grains, the carriers will tend to transport through the Ag particles in their role as bypasses, resulting in a significant reduction of S. From the BSE observation, roughly two kinds of Ag particle size are found: one less than 2 μm and the other several μm in size, which is as large as Co349 grains. Although it is difficult to quantitatively estimate the density of these two kinds of particles from the BSE images, it can be seen that the density of the agglomerated Ag particles increases with increasing Ag content. Therefore, it may be supposed that metallic conduction is dominant in CA-20 due to the large Ag agglomerate, whereas the small, dispersed Ag particles in CA-5 and CA-10 seem not to disturb the thermoelectric effect of the Co349 grains.

The thermoelectric power factor ($PF = S^2/\rho$) was calculated from measured ρ and S values (Fig. 6). The PF of each sample increases with increasing temperature. Because the addition of Ag to Co349 reduces ρ and S simultaneously, the PF of CA-5 is as high as that of CA-0. Moreover, the PF of CA-20 is about half the value of CA-0 because of the significant decrease in S. In CA-10, on the other hand, the considerable reduction

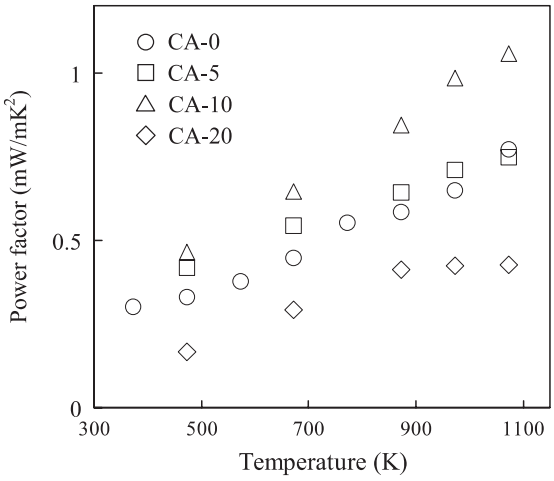

Fig. 6. T dependence of PF along the pressed plane of hot-forged Co349 and Co349/Ag samples.

of ρ, without the serious deterioration in S, enhances PF. The PF of CA-10 reaches $1\,mW/mK^2$ at 1073 K, which is the highest value from a Co349 bulk material.

4. Conclusions

Co349/Ag composites with different Ag content were synthesized by a hot-forging method using mixtures of large-grained Co349 several μm in size and submicron Ag_2O powder. Because of the lower ρ and S of Ag compared to Co349, ρ and S were simultaneously reduced by the Ag addition. The appropriate amount of Ag to improve PF was found to be 10 wt%, because it provides a significant reduction of ρ without no serious deterioration of S. Since Ag has a κ value two orders higher than that of Co349, the κ of a composite needs to be measured in order to assess the effect of the Ag addition on Z. Nevertheless, if we have a fixed temperature difference and ignore the conversion efficiency, a high-power thermoelectric device could be fabricated using Co349/Ag composite material.

References

[1] I. Terasaki, Y. Sasago, K. Uchinokura, Phys. Rev. B 56 (1997) 12,685–12,687.
[2] K. Fujita, T. Mochida, K. Nakamura, Jpn. J. Appl. Phys. 40 (2001) 4644–4647.
[3] S. Li, R. Funahashi, I. Matsubara, K. Ueno, H. Yamada, J. Mater. Chem. 9 (1999) 1659–1660.
[4] R. Funahashi, I. Matsubara, H. Ikuta, T. Takeuchi, U. Mizutani, S. Sodeoka, Jpn. J. Appl. Phys. 39 (2000) L1127–L1129.
[5] M. Shikano, R. Funahashi, Appl. Phys. Lett. 82 (2003) 1851–1853.
[6] A.C. Masset, C. Michel, A. Maignan, M. Hervieu, O. Toulemonde, F. Studer, B. Raveau, Phys. Rev. B 62 (2000) 166–175.
[7] S. Li, R. Funahashi, I. Matsubara, K. Ueno, S. Sodeoka, H. Yamada, Chem. Mater. 12 (2000) 2424–2427.
[8] D. Wang, L. Chen, S. Bai, J. Li, J. Inorg. Mater. 19 (2004) 1329–1333.
[9] D. Wang, L. Chen, Q. Wang, J. Li, J. Alloys Compd. 376 (2004) 58–61.
[10] D. Wang, L. Chen, Q. Yao, J. Li, Solid State Commun. 129 (2004) 615–618.
[11] Y. Masuda, D. Nagahama, H. Itahara, T. Tani, W.S. Seo, K. Koumoto, J. Mater. Chem. 13 (2003) 1094–1099.
[12] T. Tani, H. Itahara, C. Xia, J. Sugiyama, J. Mater. Chem. 13 (2003) 1865–1867.
[13] H. Itahara, C. Xia, J. Sugiyama, T. Tani, J. Mater. Chem. 14 (2004) 61–66.
[14] M. Sano, S. Horii, I. Matsubara, R. Funahashi, M. Shikano, J. Shimoyama, K. Kishio, Jpn. J. Appl. Phys. 42 (2003) L198–L200.
[15] Y. Zhou, I. Matsubara, S. Horii, T. Takeuchi, R. Funahashi, M. Shikano, J. Shimoyama, K. Kishio, W. Shin, N. Izu, N. Murayama, J. Appl. Phys. 93 (2003) 2653–2658.
[16] S. Horii, I. Matsubara, M. Sano, K. Fujie, M. Suzuki, R. Funahashi, M. Shikano, W. Shin, N. Murayama, J. Shimoyama, K. Kishio, Jpn. J. Appl. Phys. 42 (2003) 7018–7022.
[17] R. Funahashi, S. Urata, T. Sano, M. Kitawaki, J. Mater. Res. 18 (2003) 1646–1651.
[18] M. Mikami, E. Guilmeau, R. Funahashi, K. Chong, D. Chateigner, Proceedings of 23rd International Conference on Thermoelectrics, in press.
[19] M. Ito, D. Furumoto, S. Katsuyama, S. Hara, Proceedings of 23rd International Conference on Thermoelectrics, in press.
[20] J. Shimoyama, S. Horii, K. Otzschi, M. Sano, K. Kishio, Jpn. J. Appl. Phys. 42 (2003) L194–L197.
[21] M. Karppinen, H. Fjellvåg, T. Konno, Y. Morita, T. Motohashi, H. Yamauchi, Chem. Mater. 16 (2004) 2790–2793.